Journal of Structural Geology, Vol. 15, No. 6, pp. 785 to 792, 1993
Printed in Great Britain

0191-8141/93 $06.00+0.00

Conical folds produced by dome and basin fold interference and their application to determining strain: examples from North Canterbury, New Zealand

ANDREW NICOL *

Geology Department, University of Canterbury, Christchurch, New Zealand

(*Received* 6 *August* 1991; *accepted in revised form* 28 *July* 1992)

Abstract—Conical folds associated with dome and basin interference are analysed using equal-area plots, which provide data on the geometry of the fold surface and estimates of the finite shortening. To describe individual folds, they are subdivided into subareas defining the domains of each interfering fold set. The resulting plots demonstrate that numerous partial cones of distinct geometry are required to adequately describe the folded surface. To help identify the presence and accurately determine the geometries of such folds, the expected variations in conical fold geometry for interfering folds with varying hinge curvature, tightness and limb dips are analysed and illustrated with examples from North Canterbury. The resulting cone geometries are complex and often difficult to detect, which may in part explain the apparent absence of conical folds in some areas of dome and basin interference. Where parallel folds interfere, the divergence of poles to the conical fold surface and cone apical angle provide estimates of the finite shortening associated with folding. These shortening estimates are consistently larger than those determined by constructing profiles parallel to shortening along the hinge line of the second fold set.

INTRODUCTION

CONICAL folds commonly develop due to dome and basin fold interference (Ramsay 1962, Wilson 1967, Systra & Skornyakova 1980). Where the geometries of these interference structures are variable the resulting conical folds will be similarly diverse and bedding orientation data scattered. Consequently individual folds may have complex geometries defined by several cones. In these circumstances the presence of conical folds may be overlooked and the opportunity to define accurately the fold geometry lost.

It is informative to identify conical folds as, unlike many non-cylindrical folds, they are easy to define geometrically with the aid of stereographic or equal-area projections and may provide estimates of finite shortening. A folded surface defined by a mathematical cone must have its geometric axis oblique to the surface (Haman 1961, Stauffer 1964, Systra & Skornyakova 1980). The orientation and curvature of a conical fold surface can be defined by the inclination of the cone axis and the angle between this axis and the folded surface (Fig. 1a), which is half the apical angle of the cone (cylindrical folds may be regarded as conical folds with an apical angle equal to zero). These parameters are

*Present address: Fault Analysis Group, Department of Earth Sciences, University of Liverpool, P.O. Box 147, Liverpool L69 3BX, U.K.

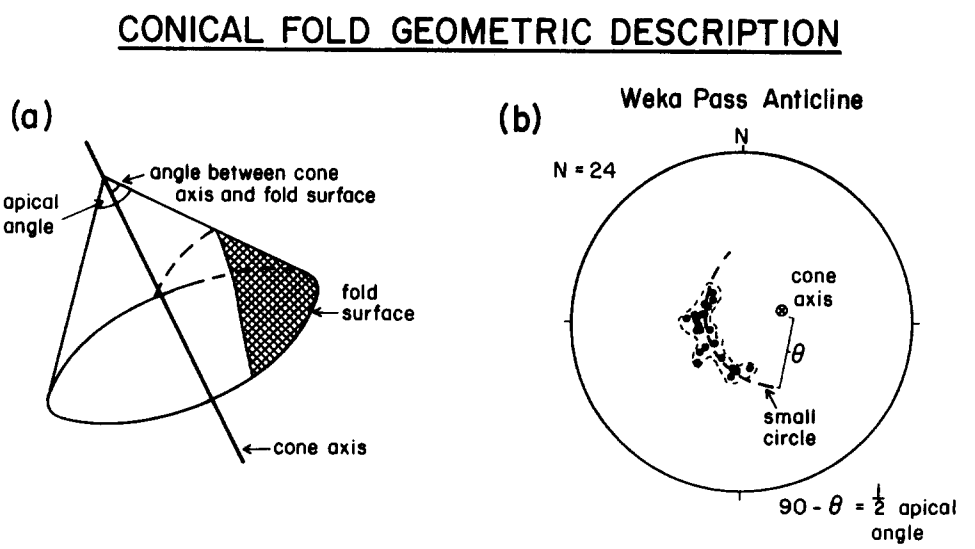

Fig. 1. Geometric description of conical fold surfaces. (a) Cone shape and geometric elements, including cone axis and apical angle, for the Weka Pass Anticline, North Canterbury. (b) The same structure represented in an equal-area plot of poles to bedding.

measured directly from equal-area plots of poles to the folded surface (bedding in the cases illustrated), which are distributed along small circles (Fig. 1b). The relative shortening associated with each of the interfering fold sets can be estimated using the cone apical angle and divergence of poles to the fold surface.

The purpose of this paper is to model complex conical fold surface geometries (developed in association with dome and basin interference patterns) by analysing the expected changes in conical fold geometry for variations in the morphology of the interfering fold sets. Domainal treatment of the folding allows the conical fold surfaces to be identified, geometrically described and the inhomogeneous shortening estimated. Examples from North Canterbury, New Zealand, provide illustration.

NORTH CANTERBURY FOLDS

Data are provided by analysis of complex early Pleistocene to recent dome and basin interference folds formed adjacent to the New Zealand plate boundary (Fig. 2). Folding, principally by buckling and flexural-slip, is developed in a strongly anisotropic sedimentary sequence of late Cretaceous to Tertiary rocks, which rest unconformably on multiply deformed Mesozoic greywacke basement. Laterally continuous Oligocene limestone units in the middle of the cover sequence form resistant ridges and dip slopes, which allow the fold geometries to be accurately defined. The two orthogonal fold sets (Fig. 2) are mainly open to gentle, with steep axial surfaces and angular, gently-plunging hinges. Fold dimensions are variable, amplitudes and wavelengths ranging from 0.05 to 1.5 km and from 1.5 to 5.9 km, respectively. Typically fold surfaces are characterized by several cone geometries with steeply inclined cone axes (60–80°), and large apical angles (ranging from 100 to 130°), locally reduced to 30–60° in the MacDonald Syncline. Folding appears to have developed in response to reverse faulting and thrusting in basement. The surface displacements of the faults are small in comparison to the fold amplitudes, and folding provides the best means of determining the finite strain.

VARIATIONS IN CONE GEOMETRY

Conical folds vary in geometry both across and along interfering fold sets. This variation directly relates to changes in the curvature of the hinge zones, fold tightness and limb dips of the interfering fold sets. These features are first discussed separately, although their effect is cumulative. Where possible, fold surfaces influenced by fold terminations have been excluded from the North Canterbury examples.

Hinge zone curvature

Upright folds usually display a reduction in dip of the fold surface towards their hinge. The interference of two folds at a high angle to each other results in a reduction in dip of the fold surface towards dome and basin structures. Figure 3(a) depicts the expected change in

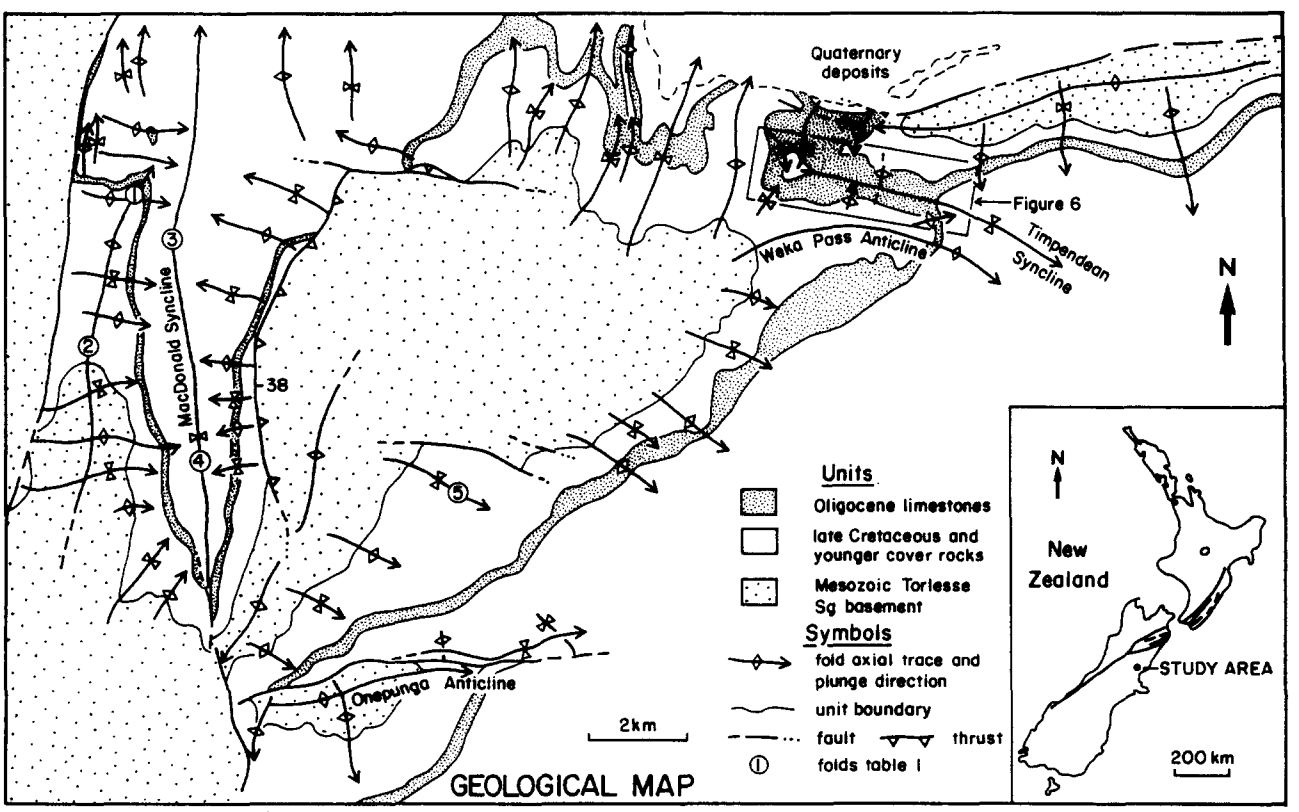

Fig. 2. Simplified geological map of the area from which all conical fold observations are drawn. Folding is emphasized by the outcrop pattern of Oligocene limestone units.

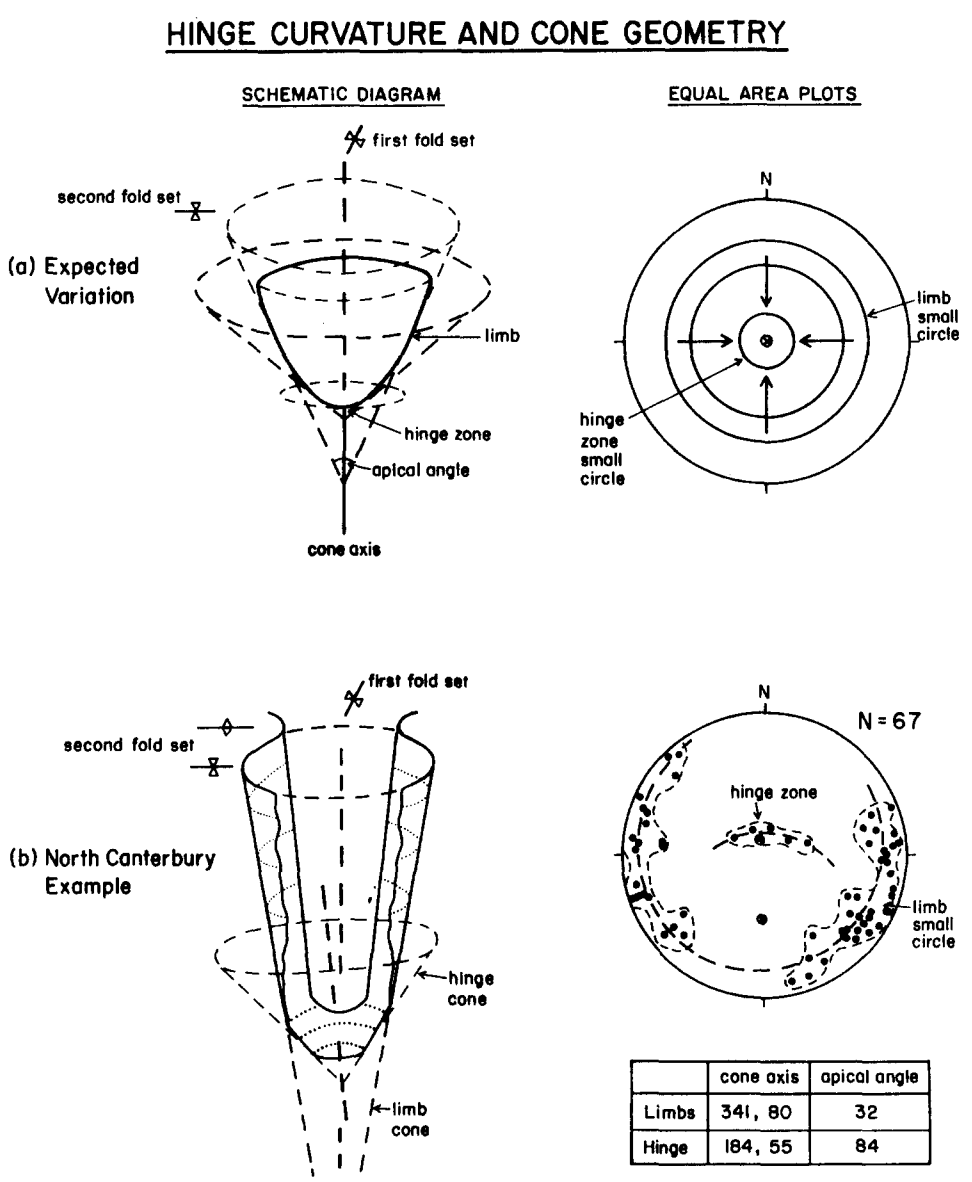

Fig. 3. Schematic diagrams and equal-area plots demonstrate the expected (a) and observed (b) changes in cone geometry towards a fold interference basin structure. The arrows on the upper equal-area net indicate the reduction in small circle size, defined by the poles to the folded surface, into the basin.

cone geometry and distribution of poles to the fold surface into a rounded fold interference basin. As limb dips decrease towards the basin (or dome) the apical angle of a cone which describes the fold surface (marked by the heavy line in Fig. 3a, schematic diagram) must increase and the small circle distribution of poles describing the cone decrease in diameter (Fig. 3a, equal-area plot). When rounded folds interfere the cone apical angle must change continuously and many cones are required to describe the surface geometry. Angular folds, such as the ones developed in North Canterbury, prove much easier to describe and the number of cones required to approximate the fold surface curvature (evident from the equal-area plots), imparted by the interfering hinge zones, is limited to one or two (Fig. 3b). Measurements on the fold surface are often not possible in hinge zones, consequently the effects of hinge zone curvature on cone geometries are often underrepresented in equal-area plots.

Fold set tightness

The ratios of fold amplitudes to wavelengths and the associated tightness of respective fold sets have a profound effect on the fold interference cone geometry. Figure 4 demonstrates the expected change in cone geometry with different combinations of fold set interlimb angles. Only if both fold sets are upright and have similar interlimb angles does the resulting cone have an apical angle approximately equal to the interlimb angles, with a steep cone axis and circular cross-section (Fig. 4, cones 1, 5, 8 and 10). Increasing the interlimb angles (i.e. decreasing the amplitude to wavelength ratio), increases the apical angle.

When the folds are upright and the interlimb angles of the interfering fold sets are different, the resulting cones become flattened (with an elliptical cross-section) perpendicular to the tightest fold set. The flattening becomes more pronounced as the difference between fold

set interlimb angles is increased, and is most obvious in the top row (cones 1–4) of Fig. 4. The flattened cone is best described by several partial cone surfaces with increasingly inclined axes (Fig. 4, cones 2–4). The apical angle of the cone surface approximately parallel to the tightest fold set increases and the apical angle describing the fold surface parallel to the second fold set decreases (Fig. 4, inset). Interfering folds with large differences in their interlimb angles are most accurately described by several cone surfaces, but will be approximately periclinal and exhibit short, cylindrical middle sections, and conical terminations. The fold surfaces in the MacDonald Syncline approach this extreme (Fig, cone 4), with interlimb angles of 43° and 146°, respectively, generating steep limb cone axes and inclined hinge cone axes (Fig. 3b). This example emphasizes the cumulative effects of the fold hinge zone and interlimb angles, with small cone apical angles on the limbs and large cone apical angles in the hinge zone. As the interlimb angle of one fold set tends to 0° or 180°, the other fold set may become approximately cylindrical. Because interfering fold sets are unlikely to have identical interlimb angles 'flattened cones' with elliptical cross-sections should be common.

Limb dips

The geometry of fold interference cones become more complex when one or both of the fold sets are asymmetric. An upright asymmetric fold will exhibit variable limb dips, and when subject to interference folding will develop different cone geometries on each limb (Fig. 5). In cases where the cone axis is steep, increasing the limb dip decreases the apical angle of the conical surface describing that limb, while the converse is true for shallow cone axes. In North Canterbury however, the geometry is more complex and the steepest limb of one fold set (e.g. Fig. 5a, north limb) is often characterized by a conical surface with a steeply plunging cone axis and a relatively large apical angle, and the shallower limb (e.g. Fig. 5a, south limb) by a shallow cone axis (trending parallel to one of the fold sets), and a smaller apical angle.

COMPOSITE CONE GEOMETRIES

The recognition of conical folds is generally reliant on having a single cone geometry defined by a well exposed

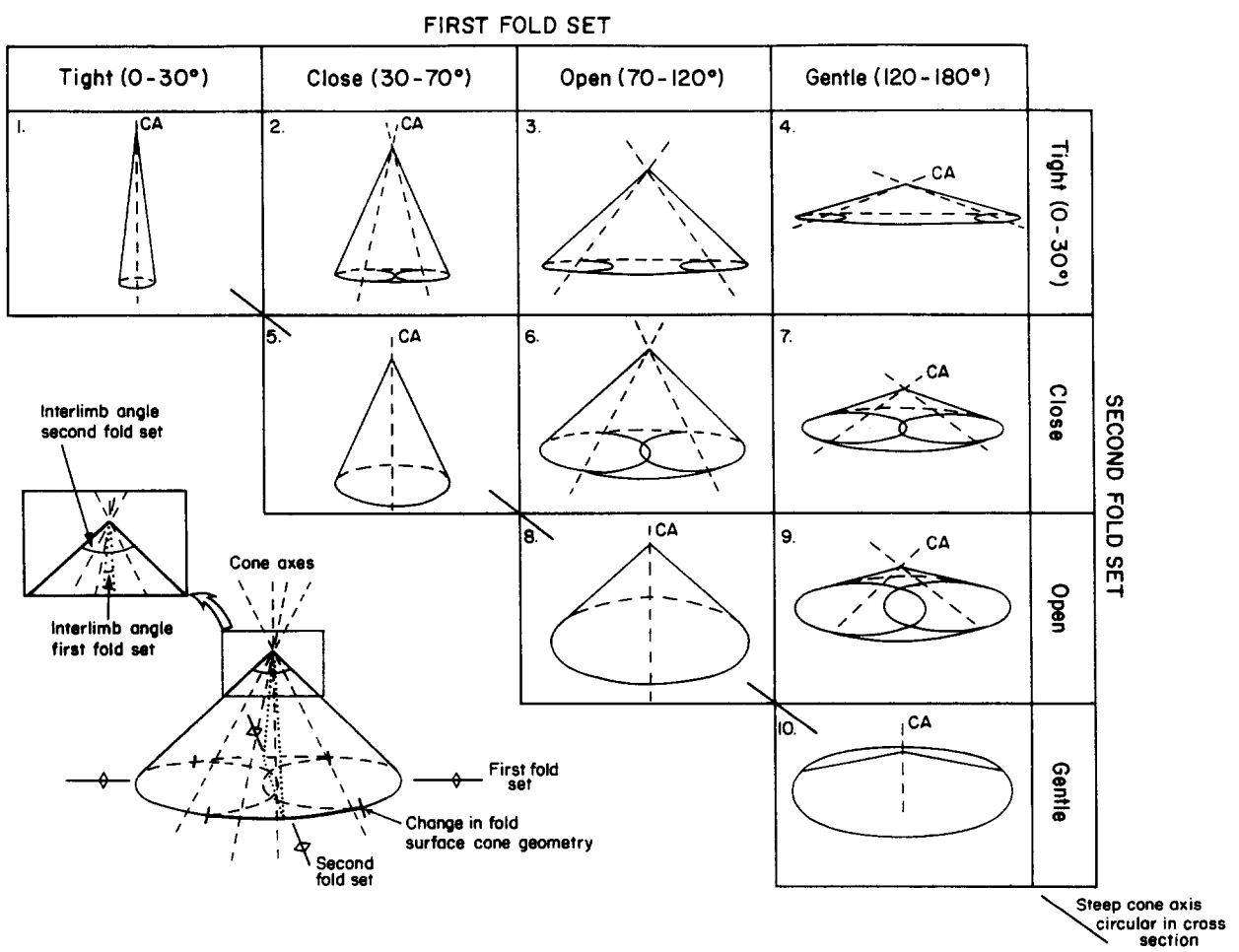

INTERFERING FOLD SET TIGHTNESS AND CHANGES IN CONE GEOMETRY

Fig. 4. Predicted changes in the geometry of conical folds produced by changes in the tightness of the interfering fold sets. These changes in the fold set interlimb angles are inferred for areas of dome and basin interference patterns where the interfering fold sets are upright and symmetrical. Hinge zone curvature effects are neglected.

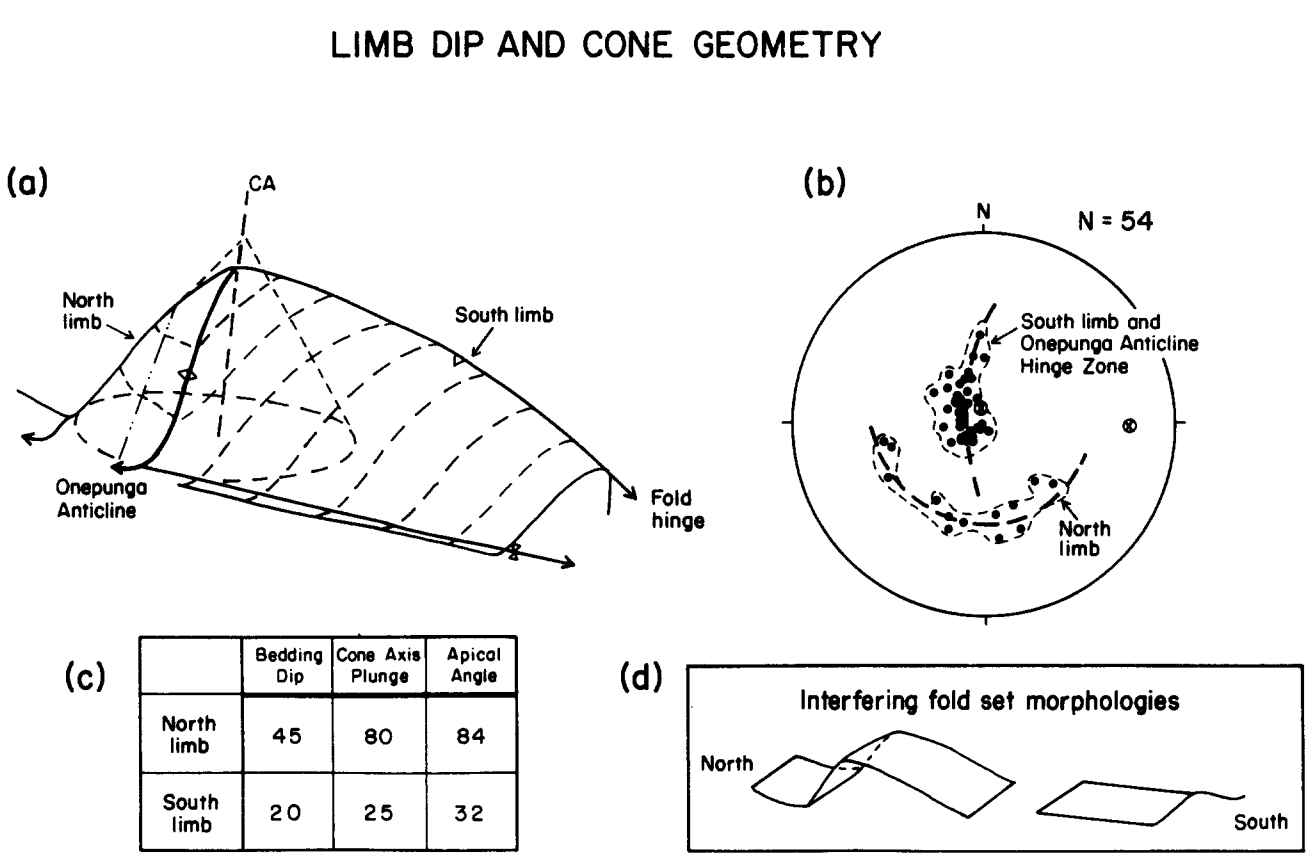

	Bedding Dip	Cone Axis Plunge	Apical Angle
North limb	45	80	84
South limb	20	25	32

Fig. 5. Variation in cone geometry with changes in limb dip for the Onepunga Anticline, North Canterbury. (a) Three-dimensional representation of the fold (with cones superimposed). (b) Equal-area plot of poles to bedding. (c) Tabulated core geometries. Inset (d) shows morphologies of the interfering fold sets.

regional fold or repeated small folds of similar geometry. However, conical fold surfaces that reflect the combined effects of interfering fold set morphologies may be irregular and apparently non-conical. The cumulative effects of these variables produce conical fold shapes that change both across and along the fold. The Timpendean Syncline (Fig. 6) provides a good example of changes in the resultant fold surface geometry due to slight variations in the morphology of the interfering fold sets. The fold surface geometry is mainly defined by cones with steep axes and large apical angles (Fig. 6), but the fold surface varies in shape from a simple conical fold (subareas 3 and 4), to a fold defined by two distinct conical surfaces (subarea 1 and possibly 2). In subarea 3 the cone apical angle is approximately equal to the Timpendean Syncline interlimb angle and reflects mainly the influence of the fold tightness. While subarea 4 appears to show the effects of a fold termination, as indicated by the reduced fold amplitude and cone apical angle. Conversely, subarea 2 is influenced by the different limb dips of the main syncline; the steeper limb has a steeper cone axis and larger apical angle than the shallower limb. Each subarea plot is limited to one or two conical segments, a function of the complexity of folding and the level of exposure in the hinge zones. If more bedding data were sampled from the hinges the distribution of poles to bedding would undoubtedly become more diffuse. Up to four distinct cone geometries have been identified in fold subareas where the hinges are well exposed (one on each limb and two describing the reduction of bedding dip into the hinge). As the number of cone geometries required to describe the fold surface increases inevitably their equal-area plots become increasingly difficult to interpret without a reduction in subarea size. For example, if all the data from the Timpendean Syncline are plotted on a single equal-area net (Fig. 6, all data), the bedding-pole distribution is more diffuse than those of the subareas, and although there is some indication that the folds are conical, both the variation and gross fold surface geometries are masked. This point is reiterated by many of the folds in North Canterbury.

Despite the continuity of the fold surface many of the equal-area plots from North Canterbury display distinctly separated and discordant bedding-pole distributions. The discontinuity between plot segments appears to coincide with angular fold hinges, which accommodate marked changes in fold surface geometry over short lateral distances.

Analytical recommendations

To recognize and adequately describe composite conical folds developed in association with dome and basin fold interference, geometrically distinct parts of the fold surface must be analysed separately. Essentially where the cones relate directly to the interfering fold sets the aim is to locate accurately the inflexion lines of each of

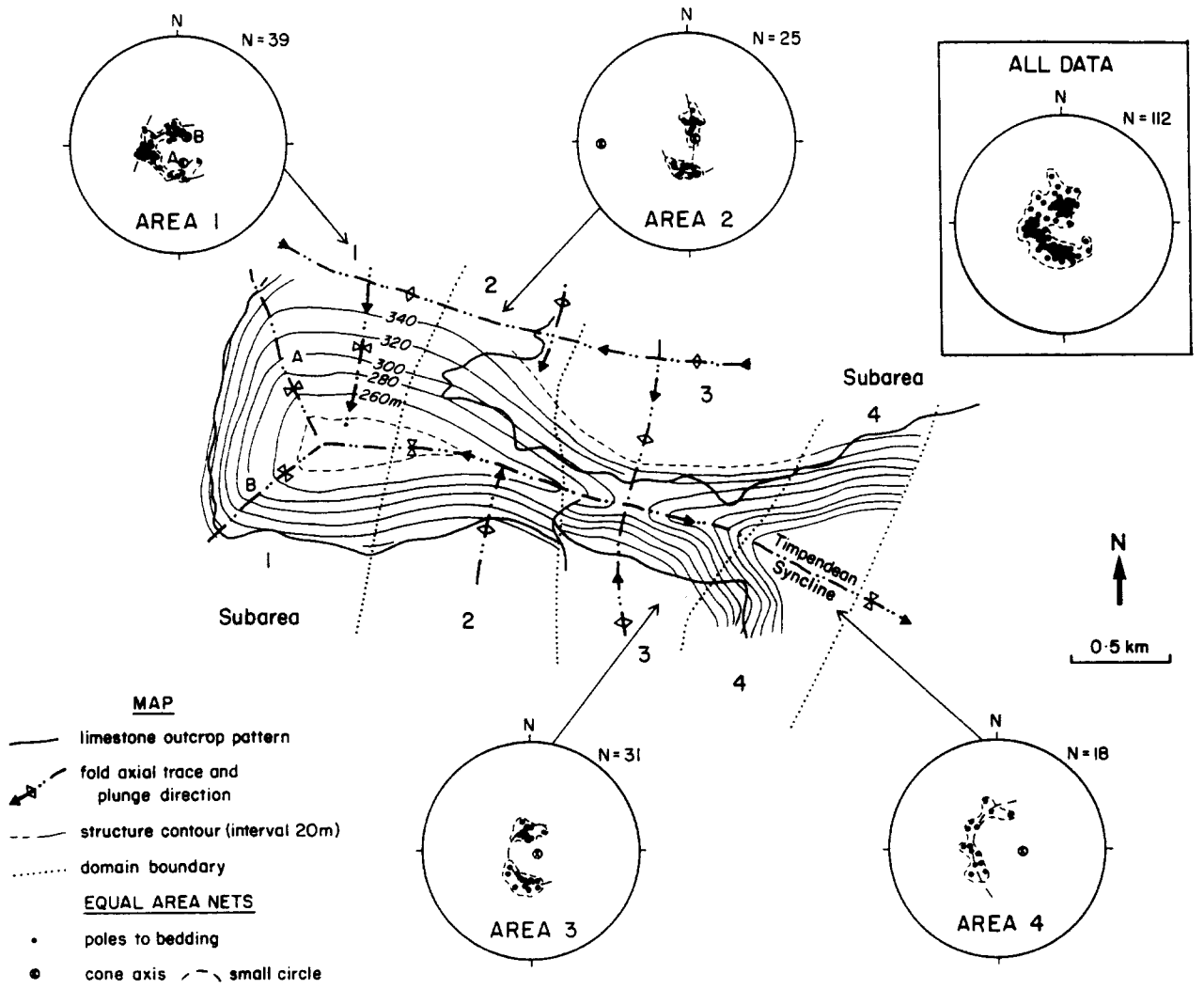

VARIATIONS IN CONICAL FOLD GEOMETRY - TIMPENDEAN SYNCLINE

Fig. 6. Map and inset equal-area nets displaying the changes in fold interference cone geometries along the Timpendean Syncline, North Canterbury. Structure contours are drawn on the mid-Oligocene paraconformity surface.

the interfering fold sets. This presents a considerable problem, particularly if the folds are rounded. Similar problems have been encountered by Turner & Weiss (1963), who recognized the need to subdivide heterogeneous folds into cylindrical fold subareas. Their solution was to place all fold data on a map and repeatedly redefine the subarea boundaries until different geometric elements, as defined by stereographic plots, are separated into discrete domains. This technique must be combined with an analysis of the changes in fold surface and axial surface orientations. Ramsay (1967) suggested two simple rules for detecting changes in fold axial orientations: (1) the strike of vertical beds is always parallel to the trend of the axial direction of folds; and (2) if beds have a dip direction which is parallel to the strike of adjacent vertical beds, then this angle of dip is equal to the angle of plunge of the fold axes. Further to this, if the cone axes are steep, lines drawn parallel to the bedding dip azimuth will tend to converge towards a common point in each subarea. In Fig. 6 placement of the subarea boundaries was helped by the angular nature of folding and inspection of structure contours, the limit of which approximately define the east–west domain boundaries. These are complemented by north–south domain boundaries, which serve as limits to the data plotted in the adjacent nets. Having crudely defined geometrically distinct portions of the fold surface it may be necessary to separate measurements from the fold hinges and limbs. This will allow the effects of the hinge zone curvatures and limb morphologies to be assessed independently and may be aided by limited exposure of the fold hinge zones. Clearly angular folds with confined hinges and straight to slightly curved limbs, formed within a brittle deformation regime, will be much more amenable to this type of analysis than rounded structures represented by compound curves. Only when the fold is divided into domains can the true geometry imposed by fold interference be determined.

Early recognition of the presence of dome and basin fold interference or irregular fold geometries may provide the key to identifying conical folds and separating out the cone geometries. Conversely, conical folds may provide an indication of previously unrecognized subtle fold interference patterns.

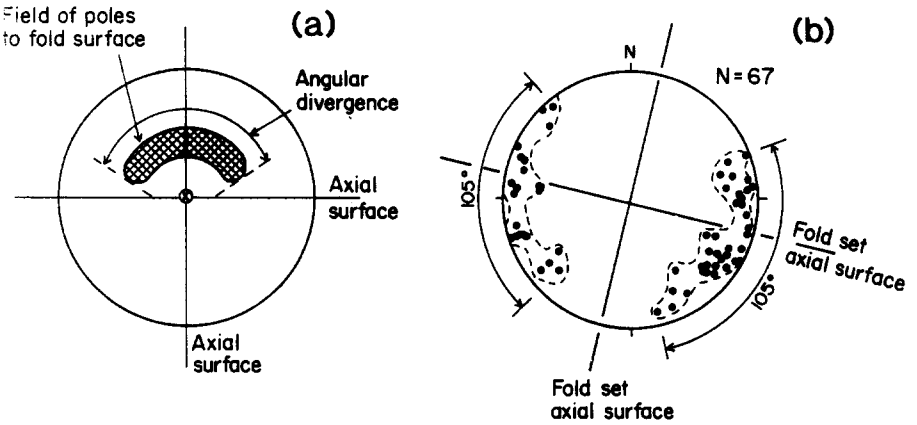

Fig. 7. Schematic diagrams illustrating the divergence of poles to conical fold surfaces and their relationship to the interfering fold axial surfaces. (a) Hypothetical situation and (b) data from the MacDonald Syncline.

CONICAL FOLD SHORTENING

Where the fold surfaces can be described by discrete cone geometries and their curvature reflects parallel folding, inhomogeneous shortening associated with the development of each fold set may be quantified directly from equal-area plots. This can be achieved in a number of special circumstances by analysing the divergence of poles to the fold surface and using the cone apical angle to estimate the fold interlimb angle.

The divergence of poles to a conical fold surface along a small circle (Fig. 7) provides a measure of the curvature of that surface. If it is assumed that the arc curvature is a product of folding of layers without signficant layer-parallel shortening, the arc to cord length ratio (Fig. 8) will provide a measure of the relative shortening imposed normal to the direction of maximum curvature. This becomes useful if the direction of maximum curvature is parallel to the axial surface of one of the interfering fold sets (Fig. 7). In effect, the distributions of poles to the fold surface must be symmetrically disposed about one or both of the axial surfaces of the interfering fold sets. Alternatively, if two concentrations of poles, one from each fold limb, rest on the same small circle (Fig. 7b) the cone apical angle is approximately equal to the interlimb of the fold set which bisects the partial small circles. The apical angle provides a means of estimating the interlimb which can be used in conjunction with the fold amplitude to determine the relative shortening.

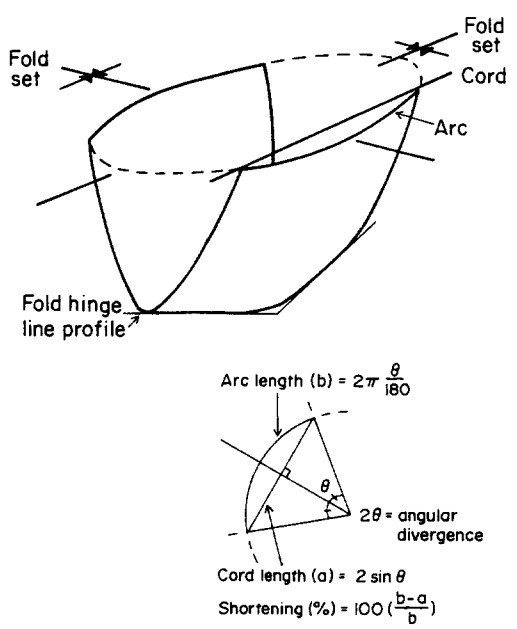

Fig. 8. Schematic diagram illustrating the relationship between interfering fold set geometries and the basis for shortening estimates derived from analysis of conical fold surfaces and hinge line profiles. Inset shows the arc–chord relationships used to derive the relative shortening estimates.

Table 1. A comparison of shortening estimates determined using the divergence of poles to conical fold surface geometry and fold hinge line profiles for six folds (located on Fig. 2) in North Canterbury

Fold	Shortening (%) Cone surface pole divergence	Fold hinge profile
1	16	14
2	15	8
3	13	8
4	16	11
5	12	6
6	9	5

In North Canterbury the divergence of fold surface poles can be used for folds where shortening estimates are between 5 and 20% (Table 1), although it is possible to determine shortening up to 36%, which is the theoretical limit of parallel folding (de Sitter 1958). For example data from the limbs of the MacDonald Syncline plot on two partial small circles (Fig. 7b). The divergence of poles on each limb is approximately 105° which implies a 16% shortening in a NNE–SSW direction (Table 1, fold 4). A more conventional method for estimating the shortening associated with the second fold set is to construct a profile along the hinge line of the first fold set. Table 1 provides a comparison of shortening estimates for six folds using conical fold surface pole divergences and fold hinge line profiles, and demonstrates that the cone geometry technique gives consistently higher values of shortening. The reason for this can be demonstrated by taking a piece of paper, which may

be regarded as representing a subarea or domain of the interfering folds (i.e. an area bounded by the inflexion lines of the interfering fold sets), and folding the paper into an upright horizontal syncline. If this fold is subsequently refolded by a syncline of similar geometry at a high angle to the first fold the ends of the paper (which were vertical after the development of the first fold), will become inclined and the horizontal distance across the second fold must decrease away from the hinge of the first fold set (Fig. 8). Therefore shortening associated with the second fold set increases from the hinge to the inflexion line (and limbs) of the first fold set. This analysis suggests that in some areas of dome and basin interference the shortening is locally variable between the hinges and limbs of the interfering fold sets.

CONCLUSIONS

Stereographic analysis of dome and basin interference folding is often regarded as being ambiguous and unrewarding because poles to the folded surface produce diffuse distributions. As shown by North Canterbury examples, interference surfaces are more commonly characterized by several cone geometries which change, both across the fold and along the hinge line. Recognition of interference folds as composite surfaces made up of conical segments with varying apical angles and cone axes allows the geometry of the folds to be described and quantified in detail. The variations in cone geometry, defined by analyses of subareas, relate directly to changes in the hinge curvature, interlimb angle and limb dips of the interfering fold sets, and therefore provide information about these characteristics. The relative shortening of each of the interfering fold sets can be determined from equal-area plots by analysing the divergence of poles around a small circle, if these are symmetrically disposed about one or both of the axial surfaces of the interfering fold sets and the folds are parallel. These estimates are consistently larger than those derived from hinge line profiles and provide a new technique for estimating shortening in areas of dome and basin interference.

Acknowledgements—This work was funded by a University of Canterbury Grants Committee research grant No. 113 9137. I wish to thank Jocelyn Campbell for many stimulating discussions and critically reviewing this paper. D. Shelley, W. Fyson, H. N. Cowan, C. W. Passchier and two anonymous referees reviewed the manuscript and provided useful comments. Lee Leonard is thanked for drafting the final figures.

REFERENCES

de Sitter, L. U. 1958. *Structural Geology*. McGraw-Hill, New York.

Haman, P. J. 1961. Manual of the stereographic projection. *West Canadian Res. Public. Calgary, Ser.* 1, *No.* 1.

Ramsay, J. G. 1962. Interference patterns produced by the superposition of folds of "similar" type. *J. Geol.* **60**, 466–481.

Ramsay, J. G. 1967. *Folding and Fracturing of Rocks*. McGraw-Hill, New York.

Stauffer, M. D. 1964. The geometry of conical folds. *N.Z. Jl. Geol. & Geophys.* **7**, 340–347.

Systra, YU. I. & Skornyakova, N. I. 1980. Conical folds in ancient complexly-folded metamorphic formations in northern Karelia. *Geotectonics* **14**, 17–25.

Turner, F. J. & Weiss, L. E. 1963. *Structural Analysis of Metamorphic Tectonites*. McGraw-Hill, New York.

Wilson, G. 1967. The geometry of cylindrical and conical folds. *Proc. geol. Ass.* **78**, 179–209.